Preprint
UCRL-JC-137819

# Line-Splitting in High-Resolution Superconducting Tunnel Junction EUV Detectors

*S. Friedrich, L. J. Hiller, M. F. Cunningham, S. E. Labov*

This article was submitted to Applied Superconductivity Conference 2000, Virginia Beach, VA, September 17-22, 2000

September 18, 2000

*U.S. Department of Energy*

Lawrence
Livermore
National
Laboratory

This work was performed under the auspices of the United States Department of Energy by the University of California, Lawrence Livermore National Laboratory under contract No. W-7405-Eng-48.

# Line-Splitting in High-Resolution Superconducting Tunnel Junction EUV Detectors

Stephan Friedrich, Lawrence J. Hiller, Mark F. Cunningham, and Simon E. Labov

***Abstract*—We have developed high-resolution Nb-Al-AlOx-Al-Nb tunnel junction extreme ultra-violet (EUV) detectors. In the energy range between 25 and 70 eV, we have measured an energy resolution of 2.2 eV full-width at half maximum (FWHM). The energy resolution degrades significantly in the energy range between ≈80 and ≈230 eV where the Nb absorber is partially transparent and some of the photons are absorbed in the Al trap layers. We have for the first time observed a distinctly different response for photons absorbed in the Nb and the Al layer of the *same* junction electrode. We have modeled this effect with Monte-Carlo simulations of the charge generation process in superconducting multilayers.**

***Index Terms*— Energy relaxation, EUV detectors, line shapes, superconducting tunnel junctions**

## INTRODUCTION

SUPERCONDUCTING tunnel junctions (STJs) have been developed over the last decade as high resolution energy-dispersive detectors for photons from optical to x-ray energies [1]. STJ detectors offer single photon efficiency and high energy resolution over a broad band at moderately high count rates.

STJ detectors utilize the small superconducting energy gap to generate about a factor 1000 more excess charge carriers (quasiparticles) upon photon absorption than conventional semiconductor detectors. This translates into a significantly higher energy resolution between 0.12 eV full-width at half maximum (FWHM) at 1 eV [2] and 8.9 eV FWHM at 1 keV [3]. STJ detectors also profit from a comparably short quasiparticle life times of order several microseconds, which allows high-resolution operation at count rates up to 10,000 counts/s [4]. Typical STJ detectors employ superconductors with different energy gaps for quasiparticle trapping to separate absorber and detector functions [5], [6]. Using a thick large gap Nb or Ta film for efficient absorption and coupling it to a thin Al tunnel junction, absorption efficiencies between 60% and 95% have been achieved.

One problem in thin-film STJ detectors using vertical trapping is that their resolution degrades at photon energies where the absorber film is partially transparent. This is because the bottom electrode of an STJ detector may have a slightly different response function from the top electrode, such that photons absorbed in it cause line broadening or even line splitting. This artifact can be avoided in STJ detectors with lateral trapping [6], which do, however, require a second detector junction for readout and must be operated at lower count rates. The artifact's influence can also be greatly reduced in STJs with a separate heavy metal absorber like Pb [7]. Most STJ detectors currently used do, however, display some line splitting artifact.

Another question is how much the response function of an STJ detector varies vertically for photons absorbed at different heights within the *same* junction electrode. This is one possible source of resolution degradation, although recent high-resolution measurements suggest that it can be made negligibly small [2].

Here, we present measurements of the EUV response of Nb-based STJ detectors. We show an unexpected line splitting into at least three lines in response to monochromatic photons in the energy range between 80 and 230 eV where the Nb absorber is partially transparent. We have modeled the line shape with spatially dependent Monte-Carlo simulations of the charge generation process in superconducting bilayers. We will also discuss the relevance of this effect for detector design and performance.

## EXPERIMENT

### A. Experimental Setup

We have developed superconducting Nb-Al-AlOx-Al-Nb EUV and X-ray detectors for high-resolution spectroscopy in astrophysics, material science and biophysics [8], [9]. They consist of a 265 nm bottom Nb film and a 50 nm bottom Al trap, which is oxidized to form a thin AlOx tunneling barrier, a top 50 nm Al trap and a 165 nm Nb absorber film. They are fabricated photolithographically on an oxidized Si sub-strate at Conductus Inc. in Sunnyvale, CA [10].

We operate these STJ detectors in a single-stage adiabatic demagnetization refrigerator (ADR) that can be attached directly to a synchrotron beam line. The ADR attains a base temperature below 0.1 K and a hold time of 8 hours below 0.5 K, the maximum operating temperature of our STJ detectors. After that, a 45-minute magnetization cycle returns the ADR to its base temperature. The ADR temperature does not need to be regulated, as the detector response in temperature independent below 0.5 K.

The low energy data shown here (25 to 70 eV) were taken at beam line 8-1, the higher energy data (above 60 eV) at beam line 1-1 of the Stanford Synchrotron Radiation Laboratory (SSRL). For measurements below 70 eV, we use three 1000 Å pure Al windows on a Ni grid to suppress noise

Manuscript received September 19, 2000. This work was performed under the auspices of the U.S. Department of Energy by University of California Lawrence Livermore National Laboratory under contract No. W-7405-Eng-48. Funding was provided by the NASA Space Astrophysics Detector Development Program grant NAG 5-4137 and the NASA High Energy Astrophysics Supporting Research and Technology Program under interagency agreement W19.121.

S. Friedrich is a physicist at the Lawrence Berkeley National Laboratory, MS 6-2100, Berkeley, CA 94720, USA. He also works as a participating guest in the Advanced Detector Group at the Lawrence Livermore National Laboratory (telephone: 510-486-7319, e-mail: SFriedrich@lbl.gov).

L. J. Hiller and M. F. Cunningham are graduate students in the Department of Applied Science at the University of California at Davis (e-mail: hiller2@llnl.gov, cunningham14@llnl.gov).

S. E. Labov leads the Advanced Detector Group at the Lawrence Livermore National Laboratory, L-418, Livermore, CA 94551, USA (telephone: 925-423-3818, e-mail: labov1@llnl.gov).

due to infrared photon absorption and to increase the ADR hold time. At higher energies, we use three 200 Å Al windows supported by 1000 Å of parylene and a Ni grid.

The photon-induced tunneling current, which provides a measure of the photon energy, is measured with a custom-designed current sensitive preamplifier with a DC voltage bias [11]. The preamplifier signal is processed with a commercial Canberra 2020 amplifier with a shaping time of 3 μs and recorded with a Nucleus multichannel analyzer.

### *B. Experimental Results*

Figure 1 shows a typical EUV spectrum for photon irradiation at 60 eV. In addition to the dominant first order line of the grating monochromator at 60 eV, higher order contributions at 120, 180 and 240 eV can also be seen (fig. 1, top). We observe a clear broadening of the detector response at 120 and 180 eV, but hardly at 240 eV. This broadening occurs at energies where the Nb absorber film is partially transparent and a significant fraction of the photons are absorbed in the Al trap. (The relative absorption efficiencies of the four films of our STJ detector are shown in fig. 1, middle.) This effect has been seen before [4], and it is well understood as being due to a somewhat different detector response from the top and bottom electrode.

One striking and unexpected result is a line splitting into at least three lines, which is most clearly resolved for 180 eV photons (fig. 1, top inset). Comparison of the line intensity ratios with the theoretical absorption efficiencies shows that the two lower-energy peaks are due to photon absorption in the top Nb and Al layer, while the higher-energy peak is due to absorption in the Nb and Al film of the counterelectrode. This agrees with the observation that the calibration of the spectrum based on the 60 and 240 eV lines, which originate from absorption in the top Nb film, places the peak assigned to the top Nb film close to 180 eV, while the peaks associated with absorption in the other films deviate from this calibration. It is possible to fit the 180 eV line complex to a four-line multiplet, but this does not improve the quality of the fit because the absorption in the bottom Nb film is too weak at this energy to be clearly resolved.

The surprising aspect of this line-splitting artifact is that the volume of charge generation upon photon absorption, also known as "hotspot", has been assumed to be much bigger than the film thickness in thin film devices such as ours [12]. Differences in absorption location throughout the Nb/Al bilayer should thus have been washed out during the initial charge generation process, since the high-energy quasiparticles and phonons of the hotspot should have spread out evenly through the bilayer well before they relax to low energies. The fact that this is apparently not the case suggests that some elements of the initial charge generation process are not yet completely understood. Below we discuss possible explanations of this line-splitting artifact.

Figure 1 also shows the measured resolution as a function of energy (bottom graph). At energies below 70 eV, the resolution is about 2.3±0.1 eV FWHM, limited by an electronic noise of 2.0 eV. At 240 eV, the resolution degrades to 4.1±0.2 eV FWHM because statistical fluctuations in the charge generation and tunneling processes are more important. The resolution is significantly reduced in the intermediate energy range where the Nb is partially transparent due to line splitting. It varies between 7.6 and 9.5 eV FWHM when fitting the multiplet to a single Gaussian. It can be improved to 4.2±0.2 eV if the fitting range is limited to just include events due to absorption in the top Nb layer.

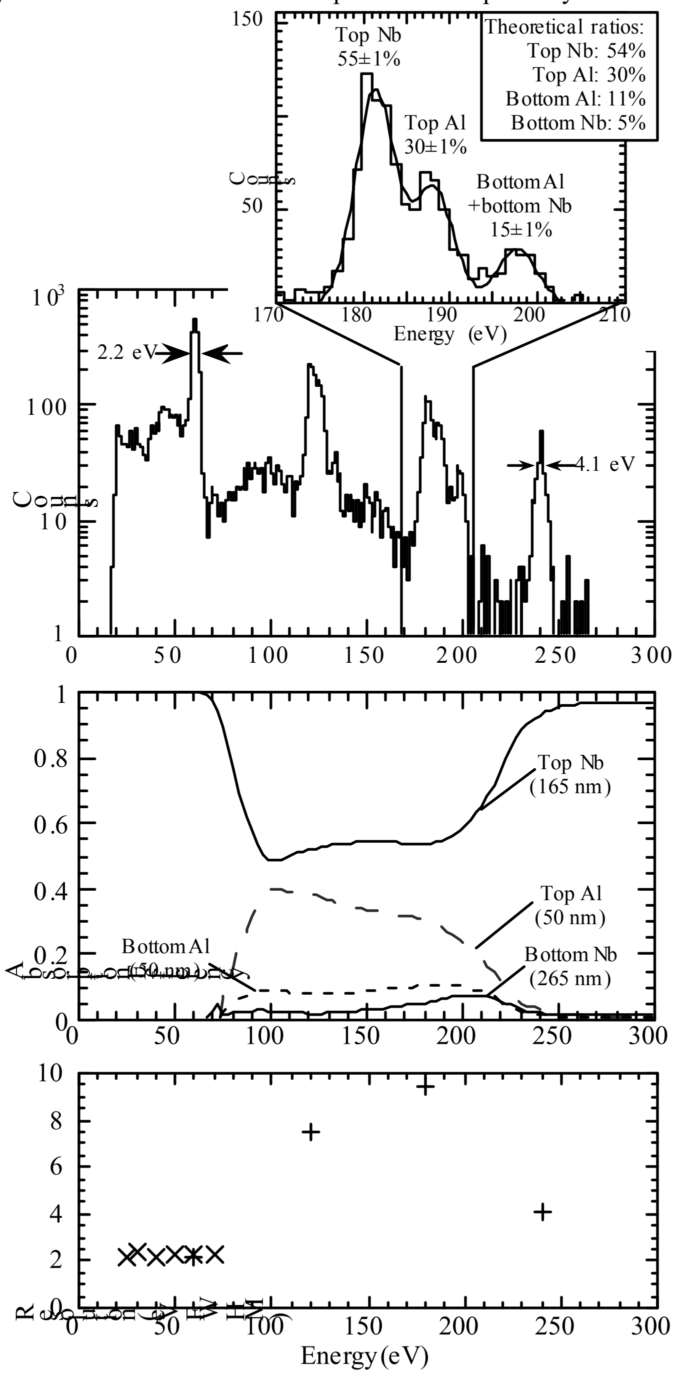


Fig. 1. STJ response to photon irradiation at 60, 120, 180 and 240 eV (top). The inset is an enlargement of the line separation in the region between 170 and 210 eV. The middle graph shows the relative absorption efficiencies of the four films of the STJ detector. The bottom graph shows resolution as a function of energy as extracted from a Gaussian fit to the lines in the above spectrum (+) and to a separate set of lower energy measurements (×). The error bars are smaller than the markers used.

## COMPUTER SIMULATIONS

### C. Charge Generation Model

The charge generation process in superconductors in response to photon absorption consists of three phases [12]. The primary photoelectron initially shares its energy through electron-electron interactions until their average energy is comparable to the Debye energy. This process dominates for about 0.1 to 1 ps depending on the superconductor and produces electrons with average energy around 0.1 eV. At that point electron-phonon scattering becomes a faster relaxation mechanism. Most electrons will thus relax by phonon emission, and for a period of about 10 to 100 ps the hotspot expands with the phonon velocity. Finally, phonons with energy above the superconducting gap $2\Delta$ will break Cooper pairs, thereby generating a measurable number of excess quasiparticles. These quasiparticles continue to relax by phonon emission and phonons will continue to break Cooper pairs until all phonon energies are below $2\Delta$. Such sub-gap phonons can no longer break Cooper pairs and will eventually escape into the substrate. The entire energy relaxation process takes about 1 ns.

Most Monte-Carlo simulations of this process are only concerned with the average energy required to generate excess quasiparticles and the associated statistical fluctuations, which determine the ultimate resolution limit of STJ detectors [13]. Therefore, they only have to consider a homogeneous superconductor, which in turn eliminates the need to simultaneously model energy relaxation and diffusion, thereby greatly reducing computational requirements. The line-splitting artifact shows that this assumption is obviously no longer satisfied in the multilayer devices discussed here.

### D. Monte-Carlo Simulations

We have performed Monte-Carlo simulations of the energy relaxation process upon photon absorption in heterogeneous superconducting multilayers [14].

Details of the initial electron-electron interaction have little relevance for the charge generation, since any information on the resulting electron distribution is lost during the subsequent cascade. We thus start our simulation with an initial set of phonons randomly distributed between zero and the Debye energy with a total energy equal to the energy of the incident photon. Each phonon with energy above $2\Delta$ is assumed to break a Cooper pair into two quasiparticles. The energies of these two quasiparticles are randomly selected, subject to energy conservation and the constraint that the average probability to create a quasiparticle with a certain energy agree with theory [15]. Each quasiparticle is then allowed to relax to a random lower energy, again constrained by energy conservation and an average relaxation probability to a certain lower energy given by theory [15]. These two processes are repeated until no phonons with energy above $2\Delta$ are left and no more Cooper pairs can be broken. The total number of quasiparticles is then recorded.

The electron mean free path is $\approx$10 nm in our Nb and (neglecting surface scattering) $\approx$60 nm in our Al films, which have a residual resistance ratio of $\approx$4. The electrons will thus undergo many elastic scattering events before scattering inelastically, thereby randomizing their vertical position in the Nb/Al bilayer between inelastic scattering events. We thus assume the electrons are evenly distributed in the bilayer and assume that scattering occurs according to the fraction of time spent in each film and the relative inelastic scattering time at the energy of the electron.

Phonons, on the other hand, have a much lower velocity and a finite transmission probability across layer interfaces [16]. In the Monte-Carlo simulation we therefore keep track of the phonon position and include reflection at the interface between dissimilar materials as well as phonon loss into the oxidized Si substrate.

The results of this simulation are summarized in table 1. The charge generated by photon absorption in the top Nb absorber is set to unity, and the charge yield from photon absorption in the other layers is normalized relative to it. Within this model, the predicted charge yield from the lower layers of the STJ detector is *less* than the yield from the top Nb layer, because high energy phonons from the lower layers are more likely to escape into the Si substrate during the relaxation process. We also note that the charge yields from photon absorption in the Nb and Al film of the *same* junction electrode are very similar, because quasiparticle transmission across the interface is assumed to be high. The results of this simulation do not agree with our observations.

### E. Line-Splitting Simulations

We have modified our Monte-Carlo simulations to assess possible causes of the observed line splitting of 3.7% between peaks originating from the top Nb and Al layers. This separation indicates that the quasiparticles (and also phonons) are not entirely free to move between the layers. In the extreme case where the charge generation process is entirely confined to the absorbing layer, the Nb and Al peaks would have a ratio of the energy gaps of 2.2. The observed line splitting suggests that a much more moderate form of confinement is present.

We examine three possible mechanisms to account for the line splitting. The first is an unexpectedly small diffusion constant, which has been observed in Ta and Al-based STJ detectors before [17]. The mean free path of $\approx$60 nm in our Al films is comparable to the 50 nm thickness of the Al trapping layer, and the corresponding elastic quasiparticle scattering time is 10 to 100 times faster than the inelastic scattering time of moderate- to high-energy quasiparticles. An impurity concentration high enough to cause confinement would be readily apparent in residual resistance ratio measurements, but this is not observed.

A second quasiparticle confinement mechanism would be a reduced quasiparticle transmission across the Al-Nb interface. The transmission due to Fermi velocity mismatch is estimated to be 85% [18]. It may be further decreased by the accumulation of residual gases on the Al trap surface during fabrication. However, the long mean free path in our Al films implies repeated attempts of the quasiparticles to cross the interface between inelastic scattering events, so confinement would be possible only with a rather small transmission coefficient. We do not believe this to be the case, since the gap values of our proximitized Al layers are well described by the Golubov model of the proximity effect

[18], which assumes good quasiparticle transmission across the Nb/Al interface, rather than the low-transmission McMillan model.

A third mechanism to account for the line splitting is a combination of some confinement plus quasiparticle loss in Nb. We observe that the top Nb layer generates smaller signals than the bottom Nb layer, despite the tendency for the bottom layer to lose phonons into the substrate. One possible loss process is quasiparticle trapping in Nb oxides. A Nb film typically forms a ≈6 nm oxide layer at an exposed surface, parts of which consist of metallic NbO [19]. This metallic surface layer can effectively trap quasiparticles and thus reduce the charge yield of the top Nb electrode relative to the bottom. However, it cannot account for the line splitting of peaks between Nb and Al layers of the *same* electrode. Some form of quasiparticle confinement is also required to shield quasiparticles in the Al from being lost in the Nb film.

We have modified our multilayer Monte Carlo simulation to examine this third mechanism. We assume that a certain fraction of the quasiparticles relaxing in the top Nb layer is completely lost into the metallic NbO layer. We also simulate confinement by not letting quasiparticles change layers between inelastic scattering events whenever their energy dependent inelastic scattering time $\tau_{in}(E)$ is shorter than some multiple of the average transit time $2d/v_{Fermi}$ they would require to traverse the film of thickness d ballistically. This ballistic approximation of diffusive motion is crude, but reduces the computational requirement considerably.

These two values were adjusted to produce the observed multiplet of figure 1. A close approximation was obtained with a loss fraction of 9.2% and a confinement condition of $\tau_{in}(E) < 2.7d/v_{Fermi}$. This means that the hotspot is confined to the layer of photon absorption until the quasiparticles have relaxed to an average energy of ≈18 meV. It also means that charge loss into the Nb oxide layer reduces the signal from events in the top Nb layer by 19.4%. The signal from events in the top Al layer is only reduced by 14.8%. The loss process has a negligible effect on charge yield from both layers of the bottom electrode. This simulation also places the weak peak originating from absorption events in the bottom Nb film at 194.1 eV (cf. fig. 1).

TABLE I
CHARGE YIELD IN EXPERIMENT AND SIMULATIONS

| Layer | Measured Signal (eV) | Measured Signal (%) | Simulated Signal No conf./loss (%) | Simulated Signal With conf./loss (%) |
|---|---|---|---|---|
| Top 165 nm Nb | 181.4 | 100 | 100 | 100 |
| Top 50 nm Al | 188.2 | 103.7 | 99.5 | 104.3 |
| Bottom 50 nm Al | 198.8 | 109.6 | 92.6 | 108.2 |
| Bottom 265 nm Nb | not resolved | | 91.5 | 107.0 |

The results of this simulation, normalized to the charge yield of the top Nb film, are summarized in the right column of table 1. Despite the crude approximations, the basic features of the multiplet are correctly identified using reasonable assumptions regarding quasiparticle loss and confinement. While metallic surface oxides constitute one possible loss mechanism in Nb, the simulation would also correctly describe other loss process like trapped flux or grain boundaries with reduced energy gap. More detailed Monte-Carlo simulations would model the diffusive quasiparticle motion during the energy relaxation process as a random walk and include the finite transparency of the Nb/Al interface.

## SUMMARY

We have developed high-resolution superconducting Nb-Al-AlOx-Al-Nb tunnel junction EUV detectors. At energies below 70 eV, they have a quantum efficiency close to unity and an energy resolution of 2.3±0.1 eV FWHM, limited so far by the electronic noise contribution of the preamplifier. In the energy range between 80 and 230 eV, where the Nb absorber film is partially transparent, we observe a line-splitting artifact of at least three distinct lines in response to monochromatic photons due to photon absorption in the Al trap layers. We have extended our Monte-Carlo simulations of the charge generation process in heterogeneous superconducting multilayers to simulate this line splitting between the Nb and the Al film of the *same* junction electrode. They suggest that this artifact is due to quasiparticle confinement during the initial stage of the charge generation process combined with quasiparticle loss in the top Nb absorber film.

## REFERENCES


[1] For a recent overview of cryogenic detector research see "*Proc. 8th Intl. Workshop on Low-Temperature Detectors (LTD-8)", Nucl. Inst. Meth.,* vol. A444, 2000

[2] P. Verhoeve, "UV/optical imaging spectroscopy with cryogenic detectors", *Nucl. Inst. Meth. A*, vol. 444, pp.435-440, 2000

[3] J.B. LeGrand et al., "A superconducting tunnel junction X-ray detector with performance limited by statistical effects", *Appl. Phys. Lett*., vol. 73, pp. 1295-1297, 1998

[4] M. Frank et al., "Energy resolution and high count rate performance of superconducting tunnel junction x-ray spectrometers", *Rev. Sci. Inst*., vol. 69, pp. 25-31, 1998

[5] N.E. Booth, "Quasiparticle trapping and the quasiparticle multiplier", *Appl. Phys. Lett*., vol. 50, pp. 293-295, 1987

[6] H. Kraus, F. v. Freilitzsch, J. Jochum, R.L. Mössbauer, T. Peterreins, F. Pröbst, "Quasiparticle trapping in a superconductive detector system exhibiting high energy and position resolution", *Phys. Lett. B* vol. 231, pp. 195-202, 1989

[7] G. Angloher et al., submitted for publication to *Appl. Phys. Lett*., 2000

[8] M. Frank et al., "Cryogenic high-resolution x-ray spectrometers for SR-XRF and microanalysis", *J. Synchrotron Rad*., vol. 5, pp. 515-517, 1998

[9] S. Friedrich et al., "Superconducting high-resolution X-ray detectors for metalloprotein L-edge spectroscopy", *J. El. Spectr. and Rel. Phenomena*, vol. 101, pp. 891-896, 1999

[10] A.T. Barfknecht, R.C. Ruby, H. Ko, "A simple and robust niobium Josephson junction integrated circuit process", *IEEE Trans. Magn*., vol. 27, pp. 3125-3128, 1991

[11] S. Friedrich et al., "Single photon imaging X-ray spectrometers using low noise current preamplifiers with dc voltage bias", *IEEE Trans. Appl. Superconductivity*, vol. 7, pp. 3383- 3386, 1997

[12] A. Zehnder, "Response of superconductive films to localized energy deposition", *Phys. Rev. B.*, vol. 52, pp. 12858-12866, 1995

[13] N. Rando et al., "The properties of Nb superconducting tunneling junctions as X-ray detectors", *Nucl. Inst. Meth. A*, vol. 313, 173-195 (1992)

[14] L.J. Hiller, "*Applications of superconducting tunnel junctions to X-ray fluorescence measurements*", Dissertation, University of California at Davis, 2000; L.J. Hiller, to be published.

[15] S.B. Kaplan, C.C. Chi, D.N. Langenberg, J.J. Chang, S. Jafarey, D. J. Scalapino, "Quasiparticle and phonon lifetimes in superconductors" *Phys. Rev. B*, vol. 14, pp. 4854-4873, 1976

[16] S.B. Kaplan, "Acoustic matching of superconducting films to substrates", *J. Low Temp. Phys*., vol. 37, pp. 343-365, 1979

[17] S. Friedrich, K. Segall, M.C. Gaidis, C.M. Wilson, D.E. Prober, A.E. Szymkowiak, S.H. Moseley, "Experimental quasiparticle dynamics in a superconducting imaging X-ray spectrometer", *Appl. Phys. Lett*., vol. 71, pp. 3901-3903, 1998; S. Friedrich, "*Superconducting single photon imaging X-ray spectrometers*", Dissertation, Yale University, 1997

[18] A.A. Golubov et al., "Proximity effect in superconductor-insulator-superconductor Josephson tunnel junctions: theory and experiment", *Phys. Rev. B*, vol. 51, pp. 1073-1089, 1995

[19] M. Grundner, J. Halbritter, "XPS and AES studies on oxide growth and oxide coatings on niobium", *J. Appl. Phys*., vol. 51, pp. 397-405, 1980